

pubs.acs.org/JPCA Article

Laser-Induced Fluorescence Spectroscopy of Large Secondary Alkoxy Radicals: Part II. Rotational and Fine Structure

Jinjun Liu,* Ming-Wei Chen, and Terry A. Miller



Cite This: J. Phys. Chem. A 2021, 125, 1402–1412



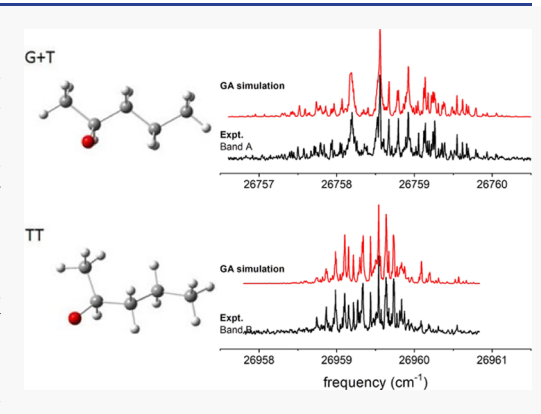
ACCESS

Metrics & More

Article Recommendations

3 Supporting Information

ABSTRACT: Selected vibronic bands of the $\tilde{B} \leftarrow \tilde{X}$ laser-induced fluorescence (LIF) spectra of jet-cooled 2-pentoxy and 2-hexoxy, including the origin and CO-stretch bands, have been measured with rotational resolution and analyzed using (1) an effective Hamiltonian that comprises a rotational part and a spin-rotation (SR) part (the "isolated-states model") and (2) a recently developed Hamiltonian in which the nearly degenerate \tilde{A} and \tilde{X} states are treated together (the "coupled-states model") (see Liu, J., J. Chem. Phys. **2018**, 148, 124112). The observed rotational and fine structures of the strongest vibronic bands have first been simulated using a genetic algorithm with the isolated-states model. The parameters for the simulation include rotational constants for both the \tilde{X} and \tilde{B} states, which can be calculated from the electronic structure theory, as well as the electronic SR constants of the \tilde{X} state and the transition dipole moments (TDMs), both of which are predicted based on their transferability in an "orbital-fixed coordinate system" using iso-propoxy as the reference molecule.



Quantum chemistry calculations suggest that the lowest two electronic (\tilde{X} and \tilde{A}) states of secondary alkoxy radicals have small energy separations on the order of 100 cm⁻¹ (see Part I of this series: *J. Phys. Chem. A* **2021**, DOI: 10.1021/acs.jpca.0c10662). The electron configurations of these two nearly degenerate states have been determined by comparing the experimentally determined rotational constants and the TDMs to the ones predicted for the \tilde{X} and \tilde{A} states. The experimental LIF spectra were also simulated with the coupled-states model, in which the effective spin—orbit (SO) constants ($a\zeta_e d$) and the SO-free separation between the \tilde{A} and the \tilde{X} states (ΔE_0) have been determined. Molecular constants derived from fitting the rotational and fine structures of the experimental LIF spectra enabled unambiguous assignment of the observed vibronic bands to specific conformers of 2-pentoxy and 2-hexoxy as reported in Part I.

1. INTRODUCTION

In the preceding paper¹ called Part I, both the moderateresolution (vibronically resolved) and high-resolution (rotationally and fine-structure resolved) laser-induced fluorescence (LIF) spectra of 2-pentoxy and 2-hexoxy are reported. Conformational identifications and vibronic assignments were made based on the comparison between the experimental LIF spectra and the ab initio calculated B-X electronic transition frequencies and B-state vibrational frequencies. The calculations confirmed that the lowest-energy conformers were observed in the experiment. In the present paper (Part II of the series), we report the prediction and simulation of the rotational and fine structure of these two molecules. The rotational analysis not only confirms the conformational and vibronic assignments reported in Part I but also provides quantitative insight into the strong vibronic interaction between the nearly degenerate \tilde{A} and \tilde{X} electronic states of these two molecules.

The current rotational analysis and simulation are based on our previous work on smaller secondary alkoxy radicals, including *iso*-propoxy and 2-butoxy. Hence, we first review previous results obtained from studying the high-resolution LIF spectra of these two molecules, as well as the cyclohexoxy radial. Historically, the rotational and fine structures of some vibronic bands of the 2-butoxy radical were first successfully simulated and assigned to two of the three conformers of the radical: G+ (with clockwise *gauche* OC2C3C4 dihedral angle) and G- (counterclockwise *gauche*).² The origin band of the third conformer, T (*trans-*), can be assigned using the principle of exclusion but cannot be simulated using the simple asymmetric top model. This is attributed to the vibronic interaction between the ground (\tilde{X}) state and the low-lying first-excited (\tilde{A}) state (at 55 cm⁻¹ for the T conformer), which is expected to strongly affect the effective electron spin-rotation (SR) constants and the resulting fine structure.

Received: November 27, 2020 Revised: January 21, 2021 Published: February 10, 2021





A breakthrough in understanding the fine structure of secondary alkoxy radicals came in 2013 when Liu et al.3 successfully simulated the rotational and fine structure of the $\tilde{B}^2A'-\tilde{X}^2A'$ origin band of iso-propoxy, the smallest secondary alkoxy. First, the standard asymmetric rotor Hamiltonian was used with quantum chemically calculated rotational constants as initial estimates. The SR constants were predicted in an "orbital-fixed coordinate system" based on the transferability of the SR tensor⁴ using ethoxy as the reference molecule.⁵ The SR constants were also calculated ab initio. 6,7 Neither the predicted nor the calculated SR constants agree with the values determined from fitting the experimental high-resolution LIF spectrum. Furthermore, the experimentally determined rotational constants are not in as good agreement with the calculated values as is the case of primary alkoxies. This is again attributed to the strong $\tilde{A} - \tilde{X}$ vibronic interaction due to a small $\tilde{A}-\tilde{X}$ separation (68 cm⁻¹). The strength of the spinorbit (SO) coupling $[-38.84 (10) \text{ cm}^{-1}]$ as well as the Coriolis coupling, compared to the SO-free A-X separation [46.6 cm⁻¹], invalidates the second-order perturbation theory commonly used to predict and calculate the SR constants, which assumes that the SR constants are dominated by the contribution from the cross-terms of the SO and the Coriolis coupling interactions in the effective Hamiltonian. 8-11 Secondorder perturbation theory predicts that SR constants of the ground electronic state have the same sign as the SO constant, which is negative for alkoxy radicals. Quite the contrary, for isopropoxy, two out of the three diagonal elements of the SR tensor (ε_{aa} and ε_{cc}) are positive. (Signs of off-diagonal elements of the SR tensor cannot be determined from fitting the experimental spectra.) It is also expected from the secondorder perturbation theory that $\varepsilon_{\rm aa}$ should vanish for isopropoxy for the following reasons. The iso-propoxy radical belongs to the C_s point group, with the a principal axis perpendicular to the C_s plane. The orbital angular momentum (L) is presumed to lie within the C_s plane based on symmetry arguments. As a result, the SR tensor is not expected to have a projection onto the a axis. However, the experimentally determined ε_{aa} has an anomalously large absolute value that is comparable to the A rotational constant.

In response to the breakdown of the second-order perturbation theory for SR constants, a "coupled-two-states" model was developed in which the nearly degenerate \tilde{A} and \tilde{X} states are treated simultaneously. The SO and Coriolis coupling terms are included in the rotational effective Hamiltonian explicitly. In this coupled-states model, the $\tilde{A}-\tilde{X}$ separation is a combined effect of the SO interaction, the "difference potential," and the difference of the zero-point-energies (ZPEs) between these two electronic states. The experimental high-resolution LIF spectrum of the *iso*-propoxy radical was simulated successfully with the coupled-states model. 3,13

Later, rotationally resolved LIF spectra of the $\tilde{B}^2A'-\tilde{X}^2A''$ and $\tilde{B}^2A'-\tilde{A}^2A'$ transitions of the chair-equatorial conformer of cyclohexoxy, ¹⁴ another secondary alkoxy radical belonging to the C_s point group, were simulated and fit simultaneously using the coupled-states model. ¹⁵ The $\tilde{A}-\tilde{X}$ separation is only 61.3307 (4) cm⁻¹ for cyclohexoxy, determined in the fit. The combined simulation and fitting of the $\tilde{B}^2A'-\tilde{X}^2A''$ and $\tilde{B}^2A'-\tilde{A}^2A'$ origin bands of cyclohexoxy further validates the new spectroscopic model. It is worth noting that neither transition frequencies nor transition intensities of the high-resolution LIF spectra of cyclohexoxy can be reproduced using the isolated-

states model, 14 in which the SO and Coriolis interactions between the \tilde{A} and \tilde{X} states are "absorbed" in the effective SR constants.

The coupled-states model was originally developed for molecules with a C_s symmetry plane like iso-propoxy and cyclohexoxy. For these molecules, the components of SO and Coriolis coupling terms that are perpendicular to the C_s plane do not affect the rotational and fine structure and, hence, vanish in the effective Hamiltonian. For molecules belonging to the C_1 group (without a symmetry element), all three components of the SO and Coriolis interactions have to be taken into account, which further complicates the effective Hamiltonian. In 2018, the coupled-states model was generalized to treat molecules without any symmetry restrictions (C₁ molecules). ¹⁶ The SO and Coriolis interactions are modeled in the internal-axis system (IAS), ¹⁷ in which the orbital angular momentum (L) and the vibrational angular momentum (G) are assumed to be along the CO bond orientation, defined as the z' axis. A transform from the IAS to the principal-axis system (PAS) involves the two orientation angles (θ and ϕ) of the CO bond in the PAS.

In a recent paper by our groups, 18 the generalized coupledstates model was used to simulate and fit the previously reported, high-resolution LIF spectra of primary 5,19,20 and secondary^{2,3} alkoxy radicals with four or fewer carbon atoms. With the exception of the T conformer of 2-butoxy, these spectra had been analyzed with the traditional "isolated-states model," in which the nearly degenerate A and X states are treated separately, whereas in the new fits using the coupledstates model, the SO and Coriolis coupling interactions are separated. The high-resolution LIF spectrum of the T conformer of 2-butoxy could not be reproduced using the isolated-states model but has been simulated using the coupled-states model with high quality. The new simulation using the coupled-states model unravels the mechanism of interactions between the \tilde{A} and \tilde{X} states. The interstate coupling constants, including the effective SO constant ($a\zeta_e d$), the Coriolis coupling constant (ζ_t) , and the SO-free $\tilde{A}-\tilde{X}$ separation (ΔE_0), determined in fitting the high-resolution LIF spectra, demonstrate a dependence on the sizes and conformations of alkoxy radicals.

In the present paper, both the isolated-states model and the coupled-states model will be applied to simulate and fit the high-resolution LIF spectra of 1-pentoxy and 1-hexoxy. The rest of this article is organized as follows: We first present a prediction of the SR constants and transition dipole moments (TDMs) of 2-pentoxy and 2-hexoxy (Section 2), followed by a presentation of both spectroscopic models (Section 3). The rotational and fine structures of the high-resolution LIF spectra were first simulated with the isolated-states model, followed by a least-squares fit to the transition frequencies (Section 4.1). To improve the quality of fitting, the high-resolution spectra were then fit using a genetic algorithm (GA) that simulates the intensity profiles (Section 4.2). Finally, the spectra were fit with the coupled-states model to extract the values for interstate-coupling constants (Section 4.3). The fit results are presented in Section 5. In Section 6, we will discuss the implications of the fit values of the molecular parameters through comparison with calculated results and with those of smaller secondary alkoxies. We will also discuss the limitations of the current spectral simulation and analysis.

Table 1. Comparison between the Molecular Parameters of 2-Pentoxy Derived in GA Fitting and the Quantum Chemically Calculated Ones (in cm⁻¹)

	G+T			TT		
	cal. ^{a,b}		expt. ^c	cal. ^{a,b}		expt. ^c
	oop	ip	type I	оор	ip	type II
A	0.26284 [3.8]	0.25428 [0.4]	0.25327 (40)	0.23424 [0.1]	0.23794 [1.7]	0.23400 (95)
B	0.05699 [-3.3]	0.05714 [-3.1]	0.05896 (14)	0.05939 [-1.8]	0.05799 [-4.1]	0.06049 (35)
C	0.05039 [-5.6]	0.05003 [-6.3]	0.05339 (14)	0.05108 [-2.1]	0.04995 [-4.2]	0.05215 (34)
$arepsilon_{aa}$	0.1069 {2.1}	0.1105 {2.1}	0.0520 (20)	0.0054 {-0.2}	-0.0176 {0.7}	-0.0252 (25)
$arepsilon_{ m bb}$	-0.0241 {0.7}	-0.0291 {0.8}	-0.0366 (8)	-0.0085 {0.6}	-0.0050 {0.4}	-0.0139 (19)
$arepsilon_{ m cc}$	0.0134 {0.7}	0.0162 {0.8}	0.0197 (8)	0.0189 {2.6}	0.0206 {2.9}	0.0072 (16)
A	1.000	0.002	0.000	1.000	0.008	1.000
В	0.741	0.003	0.523	0.073	0.003	0.178
C	0.101	1.000	1.000	0.111	1.000	0.347

^aThe numbers in square brackets represent the percent deviation of the predicted constant with respect to the fitted results. ^bThe numbers in curly brackets are the ratios between the predicted and fit values. ^cThe numbers in parentheses following the experimental values represent 1σ in the unit of the last digit.

Table 2. Comparison between the Molecular Parameters of 2-Hexoxy Derived in GA Fitting and the Quantum Chemically Calculated Ones (in cm⁻¹)

	G+TT			TTT		
	cal. ^{a,b}		expt. ^c	cal. ^{a,b}		expt. ^c
	оор	ip	type I	оор	ip	type II
A	0.23826 [-0.5]	0.23156 [-3.3]	0.23957 (59)	0.22388 [4.7]	0.21498 [0.5]	0.21385 (39)
B	0.03321 [2.3]	0.03326 [2.5]	0.03245 (13)	0.03322 [-3.7]	0.03355 [-2.8]	0.03451 (9)
C	0.03069 [5.5]	0.03060 [5.2]	0.02909 (13)	0.03057 [-2.3]	0.03054 [-2.4]	0.03128 (8)
$arepsilon_{ m aa}$	0.0198 {2.0}	0.0462 {4.7}	0.0099 (37)	1.2664 {-24.9}	-0.7662 {15.1}	-0.0509 (9)
$arepsilon_{ m bb}$	-0.0069 {-3.1}	-0.0211 {-9.5}	0.0022 (12)	-0.0270 {460.8}	0.0619 {-1056.3}	-0.0001 (1)
$arepsilon_{ m cc}$	0.0026 {-0.7}	0.0120 {-3.4}	-0.0036 (10)	-0.1543 {-27.4}	0.0464 {8.2}	0.0056 (4)
$arepsilon_{ m ab}$			-0.0201 (14)			0.0236 (7)
A	1.000	0.006	0.162	0.178	1.000	1.000
B	0.050	0.314	0.063	0.426	0.094	0.047
с	0.168	1.000	1.000	1.000	0.866	0.255

^aThe numbers in square brackets represent the percent deviation of the predicted constant with respect to the fitted results. ^bThe numbers in curly brackets are the ratios between the predicted and fit values. ^cThe numbers in parentheses following the experimental values represent 1σ in the unit of the last digit.

2. PREDICTION OF MOLECULAR PARAMETERS

To simulate the rotational and fine structures of the target molecules in their high-resolution LIF spectra, SR constants and TDMs need to be predicted and used as initial estimates in the simulation and fitting. At this stage, no *ab initio* methods are available for high-precision prediction of SR constants and TDMs of open-shell molecules in nearly degenerate electronic states such as alkoxy radicals. In the present work, they are predicted semiempirically using reference molecules. Nevertheless, these predictions require the use of *ab initio* optimized geometries and rotational constants presented in Part I.

2.1. SR Constants. In the high-resolution spectra, in addition to the rotational structure, there is the resolved fine structure that originates from the electron spin-molecular rotation interaction. SR constants of the ground electronic (\tilde{X}) state, therefore, need to be predicted as initial estimates for spectral simulation. (The SR constants of the \tilde{B} state are negligible.) In the present work, the estimations are performed using the same method as in our previous work on *iso*-propoxy, which is based on the transferability of the SR tensor upon alkyl substitution. To predict the SR constants of 2-pentoxy, *iso*-propoxy is used as the reference molecule. The transformation was done in a common "orbital-fixed"

coordinate system," which is defined as follows. The z'-axis is along the CO bond. The x'-axis is perpendicular to the z'-axis and within the plane defined by the CO-bond and the orientation of the half-filled p π orbital. The y'-axis is perpendicular to the previous two (see Figure 1 of ref 16.).

Because the electron spin is well-localized on the oxygen atom, in the common "orbital-fixed coordinate system," the "mass-independent SR tensor" defined as $\varepsilon' = I\varepsilon$, where I is the momentum of inertia tensor and ε is the SR tensor, is expected to be approximately conserved upon alkyl substitution. The SR tensor of the substituted molecules $(\varepsilon_{\rm S})$ can therefore be estimated from that of the reference molecule $(\varepsilon_{\rm R})$, iso-propoxy in the present work, using the relations 4,21

$$\varepsilon_{\mathbf{S}} = \mathbf{I}_{\mathbf{S}}^{-1} \varepsilon_{\mathbf{S}}' = \mathbf{I}_{\mathbf{S}}^{-1} \mathbf{U}_{\mathbf{S}}^{-1} \varepsilon_{\mathbf{S}}'(g) \mathbf{U}_{\mathbf{S}} = \mathbf{I}_{\mathbf{S}}^{-1} \mathbf{U}_{\mathbf{S}}^{-1} \varepsilon_{\mathbf{K}}'(g) \mathbf{U}_{\mathbf{S}}
= \mathbf{I}_{\mathbf{S}}^{-1} \mathbf{U}_{\mathbf{S}}^{-1} \mathbf{U}_{\mathbf{R}} \varepsilon_{\mathbf{K}}' \mathbf{U}_{\mathbf{R}}^{-1} \mathbf{U}_{\mathbf{S}} = \mathbf{I}_{\mathbf{S}}^{-1} \mathbf{U}_{\mathbf{S}}^{-1} \mathbf{U}_{\mathbf{R}} \mathbf{I}_{\mathbf{R}} \varepsilon_{\mathbf{R}} \mathbf{U}_{\mathbf{R}}^{-1} \mathbf{U}_{\mathbf{S}}
(1)$$

where $\mathbf{U}_{R,S}$ are the unitary transformation matrices that convert the principal coordinates, in which the momentum of inertia tensor I is diagonal, into the common coordinates (g) in which the "mass-independent SR tensor," ε' , is conserved upon substitution, that is, $\varepsilon_R'(g) = \varepsilon_S'(g)$. (Note that the difference between the actual SR tensor and the experimentally

determinable "reduced SR tensor" $\tilde{\epsilon}_S$ is neglected in the present work as has been done previously.^{4,22})

The iso-propoxy radical belongs to the C_s symmetry group with the OCH plane as the reflection plane. Its ground (\tilde{X}) and first excited (\tilde{A}) states have A' and A" symmetries, respectively. In the present work, we assume that the OCH plane of 2-pentoxy and 2-hexoxy remains a "local" C_s plane to the orbital and vibrational wave functions as in iso-propoxy, although their overall molecular symmetry belongs to the C_1 group. The half-filled p π orbital may either lie in the OCH plane or is perpendicular to it. They are labeled as "in-plane" (ip) and "out-of-the-plane" (oop) configurations (see Part I). Because of the near degeneracy of the \tilde{A} and \tilde{X} states, quantum chemistry calculations do not provide a reliable prediction as to which electron configuration gives the lower energy. Therefore, SR constants were predicted for both of the configurations, that is, for both the \tilde{X} and \tilde{A} states.

2.2. TDMs. Similar to SR tensors, the TDMs of alkoxy radicals are also closely related to the electron configurations of the two involved electronic states. Electron promotion related to the $\tilde{\mathrm{B}}\leftarrow\tilde{\mathrm{A}}/\tilde{\mathrm{X}}$ transition of the alkoxy radical is also localized to the oxygen atom. Therefore, it is reasonable to assume that the TDM is largely invariant in the "orbital-fixed coordinate system." The TDM of a substitution molecule (d_{S}) hence can be predicted from that of a reference molecule (d_{R}) , utilizing the geometry-determined unitary transformation matrices of both molecules (\mathbf{U}_{R} and \mathbf{U}_{S} as defined above)

$$d_{S} = \mathbf{U}_{S}^{-1} \mathbf{U}_{R} d_{R} \tag{2}$$

As with the SR tensors, we use *iso*-propoxy, which shows a pure c-type $\tilde{B} \leftarrow \tilde{X}$ transition, as the reference molecule to predict the TDM of 2-pentoxy, and then use 2-pentoxy as the reference molecule in the prediction of 2-hexoxy.

The predicted values for SR constants and TDMs of the G+T and TT conformers of 2-pentoxy, along with their rotational constants, are listed in Table 1, while those for the G +TT and TTT conformers of 2-hexoxy are listed in Table 2. It has been found that when comparing the two electronic configurations, ip and oop, the predicted SR tensors are similar to one another while the TDMs change significantly. This is because the switch between these two configurations corresponds to a rotation around the CO bond (the z'-axis of the "orbital-fixed coordinate system"). The components of the mass-independent SR tensor of iso-propoxy along the x'and y'-directions are comparable to each other, that is, the tensor is "near prolate." A rotation around the z'-axis, therefore, does not change the tensor greatly. The TDM, however, is a vector that forms an angle with the z'-axis and changes significantly for a rotation around it.

3. SPECTROSCOPIC MODELS

3.1. Isolated-States Model. The effective Hamiltonian of the isolated-states model used in the present work consists of two parts: the rotational part and the SR part. Other smaller terms such as that for centrifugal distortion can be neglected in simulating jet-cooled spectra because of the low rotational temperature in the jet expansion. This model has been employed in our previous work on high-resolution LIF spectra of alkoxy radicals (except methoxy^{23,24} and t-butoxy²⁵ because of their high symmetry). In brief, it can be written as

$$\mathbf{H}_{\text{eff}}^{\text{IS}} = \mathbf{H}_{\text{Rot}} + \mathbf{H}_{\text{SR}} \tag{3}$$

where H_{Rot} represents the rotational part of the Hamiltonian and H_{SR} represents the SR part. In the PAS (a, b, c)

$$\mathbf{H}_{\text{Rot}} = A\mathbf{N}_a^2 + B\mathbf{N}_b^2 + C\mathbf{N}_c^2 \tag{4}$$

in which A, B, and C are the rotational constants and N is the "spinless" rotational angular momentum, N = J - S, where J is the total angular momentum of the molecule and S is the electron spin.

The fine structure due to the coupling between the electron spin and the rotation of the molecule is modeled by the SR term $H_{SR}^{\ 22}$

$$\mathbf{H}_{SR} = \frac{1}{2} \sum_{\alpha,\beta} \varepsilon_{\alpha\beta} (N_{\alpha} S_{\beta} + N_{\beta} S_{\alpha}) \tag{5}$$

where $\varepsilon_{\alpha\beta}$ (α , β = a, b, c) are the elements of the SR tensor in the PAS.

The Hamiltonian matrix was constructed in a Hund's case (b) symmetric top basis set $|J, N, K, S\rangle$. The transition intensity formula used in this work is identical to our previous work^{5,19} and, hence, will not be repeated here.

3.2. Coupled-Two-States Model. The dominant contribution to the SR constants is *via* the cross-term of the SO interaction and the "*L*-uncoupling" term, ^{26,27} or the "Coriolis coupling term" if the vibrational angular momentum is also involved. For "Born–Oppenheimer states," for which the SO and Coriolis interactions are significantly smaller than the energy separation between the vibronic states, the numerical values of the *n*th state SR constants may be predicted by the second-order perturbation theory

$$\begin{split} \varepsilon_{\alpha\beta} &\approx \varepsilon_{\alpha\beta}^{(2)} \\ &= -\sum_{\delta} \sum_{n' \neq n} \left[\langle n' | \mu_{\alpha\delta} (L_{\delta} + G_{\delta}) | n \rangle \langle n | a L_{\beta} | n' \rangle + \langle n' | a L_{\beta} | n \rangle \right. \\ &\left. \langle n | \mu_{\alpha\delta} (L_{\delta} + G_{\delta}) | n' \rangle \right] / [E_n - E_{n'}] \end{split} \tag{6}$$

where α , β , and δ are Cartesian coordinates and μ is the effective reciprocal inertia tensor. $|n'\rangle$'s are states interacting with the nth state.

For degenerate or nearly degenerate electronic states, the second-order perturbation theory (eq 6) breaks down and does not provide a physically meaningful interpretation to the numerical values of the SR constants (see Section 4). For such states, a "coupled-two-states" model has been developed to simulate the rotational and fine structure, ¹⁶ in which the SO constant and the Coriolis coupling coefficient are used in lieu of the SR constants.

Details of the coupled-states model can be found in previous publications of our groups. ^{16,18} The Hamiltonian includes the following terms

$$\mathbf{H}_{\text{eff}}^{\text{CS}} = \mathbf{H}_{\text{q}} + \mathbf{H}_{\text{SO}} + \mathbf{H}_{\text{C}} + \mathbf{H}_{\text{Rot}} + \mathbf{H}_{\text{SR}} \tag{7}$$

where $\mathbf{H}_{\rm q}$ is the vibronic quenching Hamiltonian that gives rise to the separation of the $\tilde{\mathbf{A}}$ and $\tilde{\mathbf{X}}$ states by ΔE_0 , while $\mathbf{H}_{\rm SO}$ and $\mathbf{H}_{\rm C}$ are the SO and Coriolis coupling terms, respectively. The rotational term ($\mathbf{H}_{\rm Rot}$) and the SR term ($\mathbf{H}_{\rm SR}$) have the same forms as eqs 4 and 5, respectively. $\mathbf{H}_{\rm SO}$ and $\mathbf{H}_{\rm C}$ are constructed in the $I^{\rm r}$ representation of the PAS, (x, y, z) = (b, c, a), and can be written as

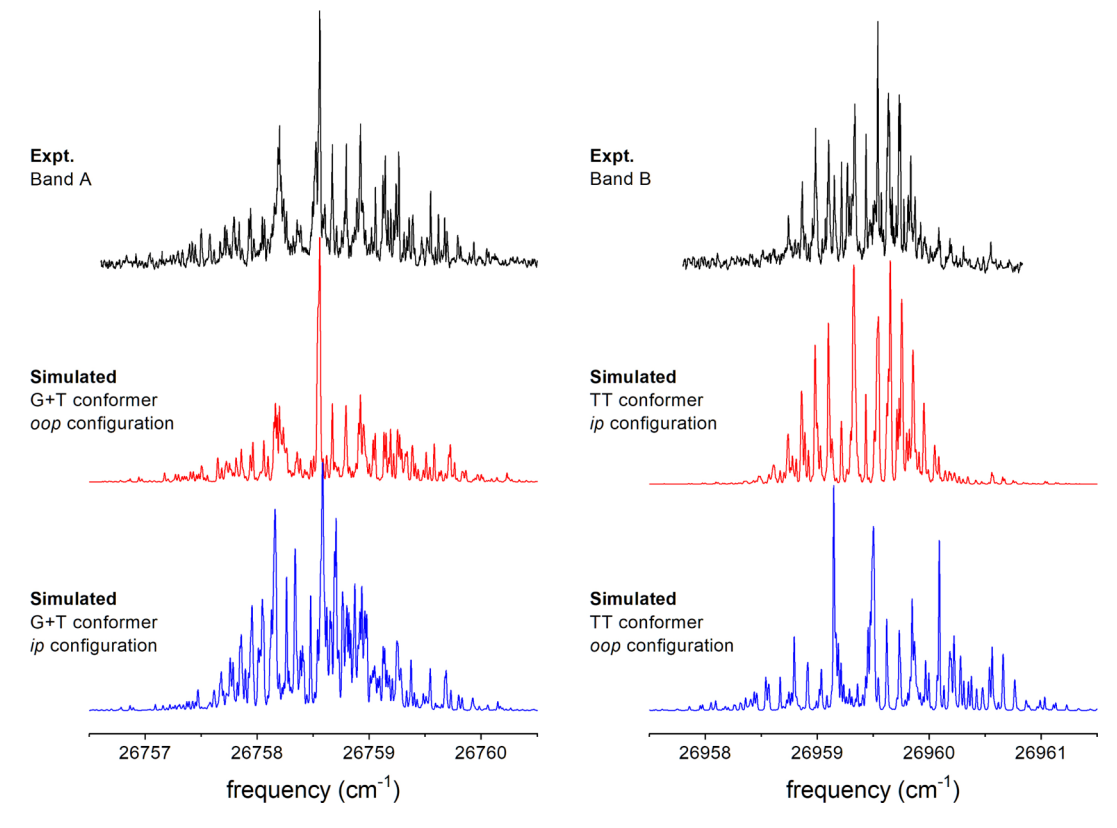


Figure 1. Experimental high-resolution LIF spectra of bands A and B of 2-pentoxy compared to simulations using predicted molecular parameters for the G+T and TT conformers, respectively. For each conformer, two sets of predicted ground-state molecular parameters corresponding to the two electronic configurations (*ip* and *oop*) are used to simulate the spectrum.

$$\mathbf{H}_{SO} = a\zeta_{e}d\mathcal{L}_{z'}(\cos\theta S_{z} + \sin\theta\cos\phi S_{x} + \sin\theta\sin\phi S_{y})$$

$$= a\zeta_{e}d\mathcal{L}_{z'}S_{z'}$$
(8)

and

$$\mathbf{H}_{C} = -2\zeta_{t} \mathcal{L}_{z'}(\cos\theta \ B_{z}N_{z} + \sin\theta \cos\phi \ B_{x}N_{x} + \sin\theta$$

$$\sin\phi \ B_{y}N_{y}) \tag{9}$$

where z' denotes the direction of L and (L + G), both of which are assumed to be along the CO bond direction in alkoxy radicals because the wave function of the unpaired electron is localized on the CO group. The polar angle of z' in the PAS, that is, the angle between the z and z' axes is denoted by θ , and the azimuth angle of z' in the PAS (with respect to x) is denoted by ϕ . (See Figure 1a of ref 16.) The expectation values of L and (L + G) in the vibronic representation are denoted by $\zeta_e d$ (vibronic quenching factor of the SO constant) and ζ_t (Coriolis coupling constant), respectively. (The expectation value of $(\hat{L} + \hat{G})$ in a vibronic state is dubbed the "Coriolis coupling coefficient," ζ_t , in distinction to the "Coriolis coefficient" or the "Coriolis constant," which involves only the vibrational angular momentum.) $\mathcal{L}_{z'}$ in eqs. 8 and 9 is the normalized or "unquenched" orbital angular momentum operator.²⁸ As discussed in ref 18, for vibrationless levels of electronic states with weak (pseudo-)Jahn-Teller interactions

$$\zeta_{t} \approx \zeta_{e} d = (a\zeta_{e} d)/a \tag{10}$$

where a is the atomic-like SO constant, ζ_e is the expectation value of the z'-axis projection of the total orbital angular momentum of the electrons, and d is the vibronic quenching

factor, viz., the Ham factor. Following previous works, 3,15,18,29,30 we assume that a is the same for the \tilde{A}/\tilde{X} -state alkoxy radicals and the ground-state OH radical $[a_{\rm OH}(\tilde{X}^2\Pi) = -139.050877 \ (41) \ {\rm cm}^{-1}]^{31,32}$ because in all cases, the unpaired electron is largely localized on the oxygen atom.

Matrix elements of the coupled-states Hamiltonian terms in eq 7 have been derived in four types of basis sets in ref 16. and included in its Supporting Information. In the present work, the totally symmetrized Hund's case (b) basis set is adopted. The overall (rotationless) $\tilde{A}-\tilde{X}$ separation contains contributions from both the SO splitting and the SO-free separation, ΔE_0 , and can be calculated as

$$\Delta E^{\tilde{A}-\tilde{X}} = \sqrt{((a\zeta_e d)^2 + \Delta E_0)^2}$$
 (11)

4. SPECTRAL SIMULATION

In the isolated-states model, 2,19 a common effective Hamiltonian for asymmetric tops is used to simulate the rotational energy level structure of alkoxy radicals. Because of the relatively small rotational constants, LIF spectra of the large secondary alkoxies studied in the present work are highly congested, which makes a definitive assignment of spectral lines difficult. The fine structure due to the SR interaction further complicates the situation. Even with the calculated rotational constants and the predicted SR constants, the assignment of the transition lines and the simulation of the spectra are arduous. To overcome the difficulty, the conventional least-square fitting of transition frequencies and the GA were combined to simulate the experimentally observed spectra.

The GA is a global optimizer that implements Darwin's natural selection principle to simulate and fit experimental data with given parameters. The readers are referred to the original literature for a detailed description of the GA (refs. 33-36) and its application to the analysis of high-resolution spectra (refs. 37,38). With GA, both the frequency and intensity information of the entire spectrum are used, and the lineshape of the spectrum is fit, instead of only the transition frequencies or intensities of individual lines as is done with conventional methods for spectral analysis. More accurate information can therefore be derived from a congested spectrum. Furthermore, GA utilizes automatic line assignment, which has a particular advantage when dealing with dense rovibrational spectra, for which spectral assignment by eye is difficult. GA is inherently a parallel procedure and can be efficiently implemented by parallel computing, which reduces the time of computation with more CPU resources. On the other hand, GA requires a rather precise calculation of rotational constants and estimation of other molecular parameters, such as TDMs, as a starting point of the fitting for a reasonable rate of convergence. In the present work, the conventional nonlinear least-squares fit typically provided a simulation in which the strongest lines are within about a full width at half-maximum from the experimental peaks before the molecular constant and spectroscopic parameters were used as initial values for GA.

Because of the strong interaction between the nearly degenerate \tilde{A} and \tilde{X} states of alkoxy radicals, the coupled-states model provides a more realistic description of the energy level structure of the molecules and can be used to derive physically more meaningful numerical values for molecular constants, especially the SO constant and the Coriolis coupling coefficient.

The simulation of transition frequencies and nonlinear least-squares fitting using either spectroscopic model were carried out using the SpecView software,³⁹ while the GA simulation was run on a Linux cluster in Nijmegen based on SUN Fire X4100 and X4150 machines.

4.1. Simulation and Fitting with the Isolated-States Model. We first simulated the high-resolution spectra of 2pentoxy using the isolated-states model with *ab initio*calculated rotational constants and predicted SR constants
and TDMs. Figure 1 shows the comparison between the
experimentally observed spectra and those simulated with the
calculated and predicted molecular parameters. For each
conformer (G+T and TT), the high-resolution spectra are
simulated with two sets of molecular parameters, corresponding to the two possible electronic configurations for the ground
state (*ip* and *oop*, see Table 2 of Part I). It is obvious that for
band A, the *oop* configuration of the G+T conformer gives a
better simulation, while for band B, the *ip* configuration of the
TT conformer gives a better simulation.

The details of the rotational and fine structure, however, are barely reproduced by the simulation using calculated and predicted molecular parameters, and a one-to-one assignment is possible only for the strongest features. Following the approach outlined above, the strongest transitions were tentatively assigned to lines in the experimentally obtained spectra, and a least-squares fitting was carried out. Since the B3LYP calculation usually gives a reliable prediction to ground-state rotational constants, ^{19,20,40} they were kept unchanged in the simulation, while other constants and parameters were adjusted and then fit to obtain the best match between the simulated and experimental spectra. Once a

good match was reached, GA was used to simulate the spectrum.

As presented in Part I, LIF spectra of 2-pentoxy and 2-hexoxy each contain vibronic bands with two types of rotational and fine structures, namely, type I and type II (see Figures 4 and 5 in Part I). Vibronic bands with different types of rotational structure are assigned to different conformers of a molecule. For both 2-pentoxy and 2-hexoxy, band A and band B belong to type I and type II rotational structures, respectively. Based on the simulations using the conventional spectroscopic method described above, type I and type II vibronic bands of 2-pentoxy are assigned to the G+T and TT conformers, respectively. For 2-hexoxy, the type I and type II vibronic bands are similar to those of 2-pentoxy and can be assigned tentatively to the G+TT and TTT conformers, respectively. Such assignments will be confirmed in the spectroscopic fitting described below.

4.2. Simulation and Fitting Using GA. To fit the highresolution spectra of 2-pentoxy with GA, the Hamiltonian of eq 3 was used. Rotational constants (A, B, and C) for both the $ilde{X}$ and $ilde{B}$ states and diagonal SR constants ($arepsilon_{aa}, arepsilon_{bb}, arepsilon_{cc}$) of the $ilde{X}$ state were involved in the GA fitting. For each molecule, all vibronic bands with the same rotational structure (type I or type II) were fit simultaneously using the same set of groundstate molecular constants. The vibronic transition frequencies of these bands were included in the fitting too. Rotational constants and SR constants of corresponding conformers determined in the conventional spectroscopic fitting (see Section 4.1) were used in the initial simulation. First, the diagonal SR constants were included in the fitting, followed by excited-state rotational constants. Ground-state rotational constants were included in the fitting later. One of the offdiagonal SR parameters, $(\varepsilon_{ab}+\varepsilon_{ba})/2$, was also included in the GA fitting of 2-hexoxy spectra since it has a significant contribution to the quality of fitting. Adding molecular constants step by step helps breaking correlation between fit parameters, especially between the ground- and excited-state rotational constants.

Several other parameters for each band were included to fit the intensity of the spectra, including the rotational temperature, $T_{\rm rot}$, and θ_{μ} and ϕ_{μ} that represent the orientation of the TDM, μ , in the PAS. The a, b, and c components of the TDMs are given by the relations

$$\mu_{a} = \mu \cos \theta_{\mu}$$

$$\mu_{b} = \mu \sin \theta_{\mu} \cos \phi_{\mu}$$

$$\mu_{c} = \mu \sin \theta_{\mu} \sin \phi_{\mu}$$
(12)

Two linewidth parameters, $\Delta \nu_L$ and $\Delta \nu_G$, for the Lorentzian and Gaussian components in the Voigt line shape function, respectively, were fixed in the fitting.

4.3. Simulation and Fitting with the Coupled-States Model. To extract quantitative information about the $\tilde{A}-\tilde{X}$ interstate coupling in 2-pentoxy and 2-hexoxy, high-resolution LIF spectra of their $\tilde{B}-\tilde{X}$ origin bands were simulated using the coupled-states model, in which the SO constants $(\zeta_{e}d)$ and SO-free $\tilde{A}-\tilde{X}$ separations (ΔE_{0}) are determined. Limited by experimental resolution, a line-to-line assignment of the rotational and fine structure can only be achieved for strong transitions. Therefore, we fix the rotational constants of both the \tilde{B} and \tilde{X} states to those determined in the GA simulation, all SR constants are set to zero, and the orientation angles of

Table 3. Molecular Parameters of 2-Pentoxy Obtained by a Fit to the High-Resolution Spectrum Using a GA

conformer	G+T			TT			
band	A	C ₁	C ₂	В	C ₃		
$ ilde{\mathbf{X}}$ State							
$A \left(\mathrm{cm}^{-1} \right)$	0.25327 (40)	0.25327 (40)	0.25327 (40)	0.23400 (95)	0.23400 (95)		
$B (cm^{-1})$	0.05896 (14)	0.05896 (14)	0.05896 (14)	0.06049 (35)	0.06049 (35)		
$C (cm^{-1})$	0.05339 (14)	0.05339 (14)	0.05339 (14)	0.05215 (34)	0.05215 (34)		
$\varepsilon_{\rm aa}~({\rm cm}^{-1})$	0.0520 (20)	0.0520 (20)	0.0520 (20)	-0.0252 (25)	-0.0252 (25)		
$\varepsilon_{\rm bb}~({\rm cm}^{-1})$	-0.0366 (8)	-0.0366 (8)	-0.0366 (8)	-0.0139 (19)	-0.0139 (19)		
$\varepsilon_{\rm cc}~({\rm cm}^{-1})$	0.0197 (8)	0.0197 (8)	0.0197 (8)	0.0072 (16)	0.0072 (16)		
		Ã	State				
$T_{00} \text{ (cm}^{-1})$	26758.3763 (10)	27312.3822 (10)	27326.4404 (10)	26959.3272 (14)	27328.5891 (11)		
$A (cm^{-1})$	0.23934 (21)	0.24101 (6)	0.23881 (16)	0.23437 (140)	0.23243 (33)		
$B \text{ (cm}^{-1})$	0.05883 (13)	0.05963 (3)	0.05970 (5)	0.05884 (27)	0.05884 (11)		
$C (cm^{-1})$	0.05304 (13)	0.05271 (3)	0.05270 (4)	0.05026 (26)	0.05025 (10)		
		Lineshap	e Parameters				
$\Delta u_{ m G} \ ({ m MHz})$	260	260	260	260	260		
$\Delta u_{ m L} \ ({ m MHz})$	150	150	150	90	90		
Weights of Transition Types							
a-type	0.000	0.773	0.479	1.000	1.000		
b-type	0.524	0.294	0.375	0.178	0.160		
c-type	1.000	1.000	1.000	0.347	0.117		
$T_{\rm rot}$ (K)	0.95	1.98	1.55	0.65	0.94		

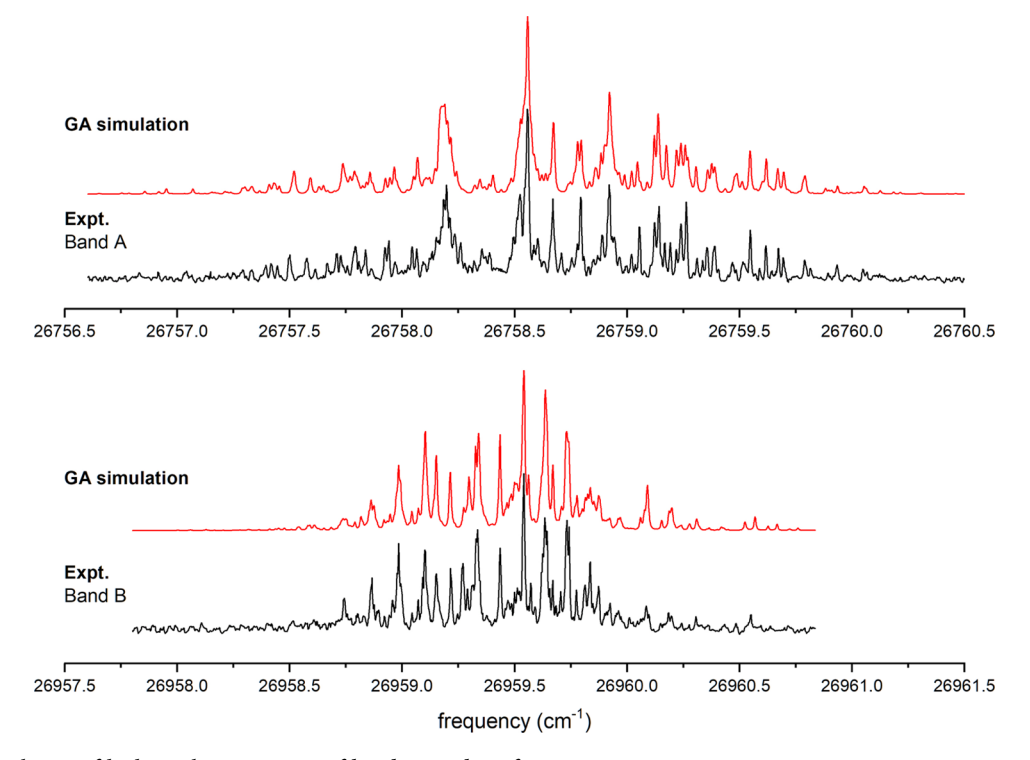


Figure 2. GA simulation of high-resolution spectra of bands A and B of 2-pentoxy.

the CO bond are set to those values calculated *ab initio*. The overall $\tilde{A}-\tilde{X}$ separations $(\Delta E^{\tilde{A}-\tilde{X}})$ of 2-pentoxy and 2-hexoxy have not been determined experimentally. In the present work, $\Delta E^{\tilde{A}-\tilde{X}}$ of the TT conformer of 2-pencoty and the TTT conformer of 2-hexoxy was fixed to that of the T conformer of 2-butoxy (55 cm⁻¹), while $\Delta E^{\tilde{A}-\tilde{X}}$ of the G+T conformer of 2-pencoty and the G+TT conformer of 2-hexoxy was fixed to that of the G+ conformer of 2-butoxy (125 cm⁻¹). We further apply the approximations that $\zeta_t = \zeta_e d$, and $\zeta_e d = (a\zeta_e d)/a_{\rm OH}$. The SO-free $\tilde{A}-\tilde{X}$ separation (ΔE_0) is related to $a\zeta_e d$ and

 $\Delta E^{\tilde{A}-\tilde{X}}$ through eq 11. Therefore, the only molecular constant in the coupled-states model that needs to be fit is the effective SO constant $a\zeta_{\rm e}d$.

5. RESULTS

The rotational and fine structures of all five non-overlapping vibronic bands of 2-pentoxy for which high-resolution LIF spectra were obtained (A, B, C_1 , C_2 , C_3) were simulated and fit using the isolated-states model with GA. The fit parameters are summarized in Table 3. The resulting simulated bands A and B

in comparison with experimental spectra are illustrated in Figure 2.

The overlapping bands D_{1-7} were simulated by adding up type II bands with adjusted band origins. The ground- and excited-state molecular constants are fixed to those of band B, although their upper-state rotational constants are expected to differ slightly. The fit center frequencies are listed in Table 6 of Part I. As an example, the comparison between the simulated and experimentally obtained bands $D_{4,5}$ is illustrated in Figure 3

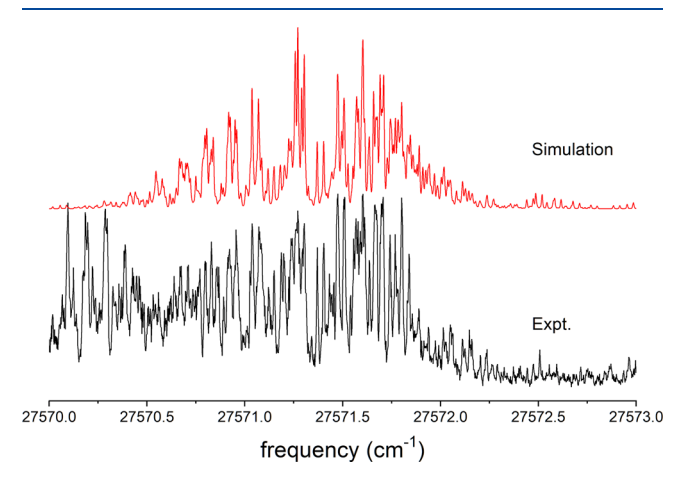


Figure 3. Simulated and experimentally obtained high-resolution spectra of bands $D_{4,5}$ of 2-pentoxy. The lowest-frequency portion of the experimental spectrum is the partially overlapping D_3 band.

Comparison between the calculated or predicted values for the molecular parameters (rotational constants and TDMs) of 2-pentoxy with those determined in fitting experimentally obtained spectra (see Table 1) confirms the conformational identification and the vibronic assignment reported in Part I. One can safely assign the type I bands to the G+T conformer and type II bands to the TT conformer.

Molecular parameter values of 2-hexoxy from fits with GA are listed in Table 4. They are compared with the calculated and predicted ones in Table 2. The agreement is not as satisfactory as for 2-pentoxy but sufficient to verify the conformational assignments. Comparison between the experimental and simulated spectra is illustrated in Figure 4.

The B-X origin bands (bands A and B) of the TT and G+T conformers of 2-pentoxy and the TTT and G+TT conformers of 2-hexoxy were simulated using the coupled-states model. Molecular constants determined in the fits with the coupled-states model are summarized in Table 5. The fit spectra are compared with the experimental ones in Figures S.1 and S.2 in the Supporting Information, respectively. The quality of the simulation is comparable to that using GA with the isolated-states model.

6. DISCUSSION

6.1. Electronic Configurations of the \tilde{A} and \tilde{X} States and Ground-State Molecular Constants. Compared with the primary alkoxy radicals, the energy separations between the \tilde{A} and \tilde{X} states of secondary alkoxy radicals are quite small. As discussed in Part I, both 2-pentoxy and 2-hexoxy radicals have nearly degenerate \tilde{A} and \tilde{X} states based on quantum chemistry calculations. Even the ZPE correction can reverse the energy ordering of these two states, for example, in the cases of the

Table 4. Molecular Parameters of 2-Hexoxy Obtained by a Fit to the High-Resolution Spectrum Using a GA

conformer	G+TT	T	ГТ					
band	A	В	D					
	$\mathbf{ ilde{X}}$ State							
$A \left(\text{cm}^{-1} \right)$	0.23957 (59)	0.21385 (39)	0.21385 (39)					
$B (cm^{-1})$	0.03245 (13)	0.03451 (9)	0.03451 (9)					
$C \text{ (cm}^{-1})$	0.02909 (13)	0.03129 (8)	0.03129 (8)					
$\varepsilon_{\rm aa}~({\rm cm}^{-1})$	0.0099 (37)	-0.0509 (9)	-0.0509(9)					
$\varepsilon_{\rm bb}~({\rm cm}^{-1})$	0.0022 (12)	-0.0001 (1)	-0.0001 (1)					
$\varepsilon_{\rm cc}~({ m cm}^{-1})$	-0.0036 (10)	0.0056 (4)	0.0056 (4)					
$(\varepsilon ab + \varepsilon ab)/2)$ (cm^{-1})	-0.0201 (14)	0.0236 (7)	0.0236 (7)					
	$ ilde{\mathbf{A}}$ State	:						
$T_{00} \text{ (cm}^{-1})$	26755.7053 (2)	26914.3129 (6)	27525.9520 (5)					
$A (cm^{-1})$	0.22057 (37)	0.21263 (33)	0.21250 (13)					
$B \left(cm^{-1} \right)$	0.03314 (12)	0.03356 (7)	0.03363 (3)					
$C (cm^{-1})$	0.02932 (12)	0.03062 (7)	0.03068 (3)					
Lineshape Parameters								
$\Delta u_{ m G} \ ({ m MHz})$	180	240	240					
$\Delta u_{ m L} \ ({ m MHz})$	150	60	60					
Weights of Transition Types								
a-type	0.162	1.000	1.000					
b-type	0.063	0.006	0.047					
c-type	1.000	0.256	0.255					
T _{rot} (K)	1.33	0.73	0.90					

G+T and the TT conformers of 2-pentoxy. Quantum chemistry calculations predict that the half-filled orbital of the ground state of both conformers lies approximately in the OCH plane, that is, the *ip* configuration, but the ZPE corrections swap the energy ordering. Experimentally, however, a better simulation is given by the *oop* configuration for the TT conformer and by the *ip* configuration for the G+T conformer.

Comparing between the calculated molecular parameters using the two different electron configurations, the most distinctive difference is between the TDMs. The *ip* configuration gives dominantly c-type transitions, while the *oop* configuration gives dominantly a-type transitions (see Table 1). Quantum chemistry calculations give different rotational constants for these two states as well, which supports the energy ordering of the electronic configurations determined based on TDMs. The most pronounced difference is in the rotational *A* constants (see Tables 1 and 2). For example, for the TT conformer, the discrepancy between the experimentally derived rotational constants and the calculated ones is about 20 times smaller for the *oop* configuration than for the *ip* configuration. For the G+T conformer, the difference is about a factor of 10.

The predicted values for SR constants are similar for the two configurations for a reason explained before (see Section 2). The predicted values for SR constants are within a factor of 2 of the experimental values in most cases. When compared with primary alkoxies 19,20,40 or related peroxy radicals, 41,42 the accuracy of the quantum chemically calculated rotational constants and the predicted SR constants is less satisfactory. A similar discrepancy has been observed for *iso*-propoxy. This is attributed to the strong interaction between the nearly degenerate \tilde{A} and \tilde{X} states and the breakdown of second-order perturbation theory.

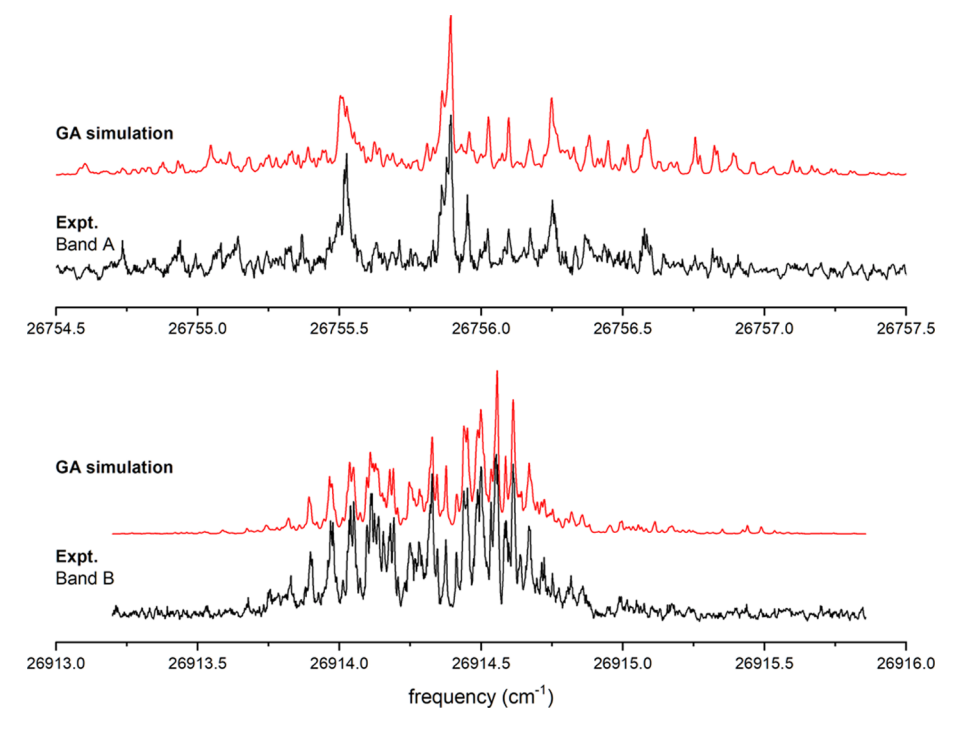


Figure 4. GA simulation of high-resolution spectra of bands A and B of 2-hexoxy.

Table 5. \tilde{A}/\tilde{X} -State Molecular Constants of 2-Pentoxy and 2-Hexoxy Determined in Fitting their Experimental High-Resolution $\tilde{B} \leftarrow \tilde{X}$ LIF Spectra Using the Coupled-States Model^a

	2-pentoxy		2-hexoxy	
	G+T	TT	G+TT	TTT
$\Delta E^{\tilde{A}-\tilde{X}}$ (cm ⁻¹)	125 ^b	55 ^c	125 ^b	55 ^c
$a\zeta_{\rm e}d~({\rm cm}^{-1})$	-53.0 (14)	-28.8(4)	-50.2(7)	-25.6 (10)
$\Delta E_0 \ (\mathrm{cm}^{-1})^d$	113.2	46.9	114.5	48.7
$\zeta_{\rm t} = \zeta_{\rm e} d$	-0.4^{e}	-0.2^{e}	-0.4^{e}	-0.2^{e}
θ (deg.)	79.9 ^f	49.4 ^f	80.4 ^f	40.2^{f}
ϕ (deg.)	20.4 ^f	16.6 ^f	25.7 ^f	8.8^{f}
T_{oo} (cm ⁻¹)	26695.88 ^g	26931.84 ^g	26693.21 ⁸	2,6886,82 ^g

"Numbers in parentheses are uncertainties in the last digit. ^bFixed to $\Delta E^{\tilde{A}-\tilde{X}}$ of the G+ conformer of 2-butoxy determined in DF measurement. ⁴⁵ "Fixed to $\Delta E^{\tilde{A}-\tilde{X}}$ of the T conformer of 2-butoxy determined in DF measurement. ⁴⁵ "Calculated from $\Delta E^{\tilde{A}-\tilde{X}}$ and the fit value of $a\zeta_e d$ using eq 11. "Calculated using the fit value of $a\zeta_e d$ and the previous experimental value of $a_{\rm OH} = -139~{\rm cm}^{-1}$. $\zeta_{\rm t} = \zeta_e d = (a\zeta_e d)/a_{\rm OH}$. Fixed to the calculated values at the B3LYP/6-31+G* level of theory. Befined as the energy between the middle point of the vibrationless levels of the \tilde{X} and \tilde{A} states and the vibrationless level of the \tilde{B} state.

6.2. GA Fitting. Because of the small rotational constants, the rotational structures in the high-resolution spectra of 2-pentoxy and 2-hexoxy are only partially resolved. GA has proved to be an effective approach for simulating high-resolution spectra and deriving molecular constants. Previously, the GA has been implemented to simulate the cavity ring-down spectra of peroxy radicals. Compared to those works, the quality of GA simulation in the present work is poorer, particularly for reproducing the transition intensities. This is not surprising. In cavity ring-down spectroscopy, the absorption intensity is determined by fitting the decay of the

ring-down curve. Therefore, the cavity ring-down technique is largely immune from power fluctuation in the laser source as long as the ring-down decay is a single exponential curve and the detection system has a linear response. The intensity of LIF, however, is proportional to the pulse intensity of the excitation laser and subject to the pulse-to-pulse power fluctuation of the laser source. The intensity reproducibility of LIF spectra, therefore, is significantly worse than that of cavity ring-down spectroscopy.

6.3. Coupled-States Model and Interstate-Coupling Constants. In Sections 4.1 and 4.2, the rotational and fine structures of 2-pentoxy and 2-hexoxy are simulated using the *effective* Hamiltonian of the isolated-states model. This model does not include explicitly the SO and Coriolis coupling terms that couple the nearly degenerate \tilde{A} and \tilde{X} states. Rather the effective (quenched) SO constant ($a\zeta_e d$) and the Coriolis coupling constant (ζ_t) are "absorbed" in the SR constants. In addition, these two interstate terms also perturb the rotational energy level structure and lead to correction terms to the (*effective*) rotational constants. ^{28,43,44} Simulations using the coupled-states model provide a more accurate representation of the mechanism that couples the two nearly degenerate states.

As Table 5 shows, the interstate-coupling constants ($a\zeta_e d$ and ΔE_0) of the G+T conformer of 2-pentoxy and the G+TT conformer of 2-hexoxy are close to those of the G+ conformer of 2-butoxy ($a\zeta_e d = -49.79 \text{ cm}^{-1} \text{ and } \Delta E_0 = 115 \text{ cm}^{-1}$). The effective SO constants ($a\zeta_e d$) of the TT conformer of 2-pentoxy and the TTT conformer of 2-hexoxy are close to each other (-28.8 and -25.6 cm⁻¹, respectively) but significantly smaller than the T conformer of 2-butoxy ($a\zeta_e d = -43.96 \text{ cm}^{-1}$). As a result, ΔE_0 of the TT and TTT conformers are larger than the T conformer of 2-hexoxy ($\Delta E_0 = 33 \text{ cm}^{-1}$). It is worth noting that in the present work, the $\tilde{A}-\tilde{X}$ separations of 2-pentoxy and 2-hexoxy are fixed to those of corresponding 2-butoxy conformers because of the lack of experimental

dispersed fluorescence (DF) spectra. Therefore, ΔE_0 determined in fitting the LIF spectra may have large uncertainties (see Discussion in ref 18.).

7. CONCLUSIONS

In this second part of the series, partially resolved rotational and fine structures in the high-resolution LIF spectra of 2-pentoxy and 2-hexoxy reported in Part I have been analyzed and simulated. Using an asymmetric top model that includes the SR interaction, the high-resolution spectra were simulated with rotational constants calculated *ab initio* and the predicted SR constants and TDMs. The predictions were made in an "orbital-fixed coordinate system" based on the transferrability of these two quantities. Comparison between simulated and experimental spectra confirms the conformational identification made in Part I. We have further used a GA approach to simulate and fit the observed high-resolution spectra and derive molecular constants.

Quantum chemistry calculations predict that the \tilde{A} and \tilde{X} states of these two secondary alkoxy radicals are nearly degenerate. It is, therefore, unreliable to determine the ground-state electron configuration from these calculations because even the ZPE corrections can alter the energy ordering. However, the electronic configuration can be determined by simulating the high-resolution spectra.

The two nearly degenerate states, \tilde{A} and \tilde{X} , are coupled by the SO and Coriolis interactions, which are not explicitly included in the traditional effective rotational Hamiltonian for an asymmetric top. Therefore, the "coupled-states model" was implemented to simulate and fit the high-resolution spectra. With this model, the effective SO constant $(a\zeta_e d)$ and the Coriolis coupling constant (ζ_t) for the lowest-energy conformers of 2-pentoxy and 2-hexoxy have been determined, which can be used to benchmark future ab initio calculations.

ASSOCIATED CONTENT

Solution Supporting Information

The Supporting Information is available free of charge at https://pubs.acs.org/doi/10.1021/acs.jpca.0c10663.

Simulation of high-resolution LIF spectra of 2-pentoxy and 2-hexoxy using the coupled-states model (PDF)

AUTHOR INFORMATION

Corresponding Author

Jinjun Liu — Department of Chemistry and Department of Physics, University of Louisville, Louisville, Kentucky 40292, United States; orcid.org/0000-0002-3968-2059; Email: j.liu@louisville.edu

Authors

Ming-Wei Chen – Department of Chemistry, The Ohio State University, Columbus, Ohio 43210, United States

Terry A. Miller — Department of Chemistry, The Ohio State University, Columbus, Ohio 43210, United States; orcid.org/0000-0003-0731-8006

01clu.01g/ 0000 0003 0/31 0000

Complete contact information is available at: https://pubs.acs.org/10.1021/acs.jpca.0c10663

Notes

The authors declare no competing financial interest.

ACKNOWLEDGMENTS

The authors are grateful to Drs. Christopher C. Carter and Sandhya Gopalakrishnan for taking the LIF spectra. This work was supported by the National Science Foundation under grant no. CHE-1454825 and CHE-1955310. T.A.M. acknowledges support from the Ohio Supercomputer *via* project no. PAS0540.

REFERENCES

- (1) Liu, J.; Miller, T. A. Laser-Induced Fluorescence Spectroscopy of Large Secondary Alkoxy Radicals. Part I. Spectral Overviews and Vibronic Analysis. *J. Phys. Chem. A* **2021**, DOI: 10.1021/acs.jp-ca.0c10662.
- (2) Stakhursky, V. L.; Zu, L.; Liu, J.; Miller, T. A. High resolution spectra and conformational analysis of 2-butoxy radical. *J. Chem. Phys.* **2006**, *125*, 094316.
- (3) Liu, J.; Melnik, D.; Miller, T. A. Rotationally resolved $\tilde{B} \leftarrow \tilde{X}$ electronic spectra of the isopropoxy radical: A comparative study. *J. Chem. Phys.* **2013**, 139, 094308.
- (4) Tarczay, G.; Gopalakrishnan, S.; Miller, T. A. Theoretical Prediction of Spectroscopic Constants of 1-Alkoxy Radicals. *J. Mol. Spectrosc.* **2003**, 220, 276.
- (5) Tan, X. Q.; Williamson, J. M.; Foster, S. C.; Miller, T. A. Rotationally resolved electronic excitation spectra of the ethoxy $\tilde{B} \leftarrow \tilde{X}$ transition. J. Phys. Chem. 1993, 97, 9311.
- (6) Gauss, J.; Kállay, M.; Neese, F. Calculation of Electronicg-Tensors using Coupled Cluster Theory†. *J. Phys. Chem. A* **2009**, *113*, 11541–11549.
- (7) Tarczay, G.; Szalay, P. G.; Gauss, J. First-Principles Calculation of Electron Spin-Rotation Tensors. *J. Phys. Chem. A* **2010**, *114*, 9246–9252
- (8) Van Vleck, J. H. The Coupling of Angular Momentum Vectors in Molecules. *Rev. Mod. Phys.* **1951**, 23, 213.
- (9) Henderson, R. S. Electron Spin Coupling in Polyatomic Molecules. *Phys. Rev.* **1955**, *100*, 723.
- (10) Curl, R. F. Microwave Spectrum of Chlorine Dioxide. III. Interpretation of the Hyperfine Coupling Constants Obtained in Terms of the Electronic Structure. *J. Chem. Phys.* **1962**, *37*, 779–784.
- (11) Curl, R. F. The relationship between electron spin rotation coupling constants andg-tensor components. *Mol. Phys.* **1965**, *9*, 585.
- (12) Mills, P. D. A.; Western, C. M.; Howard, B. J. Rotational Spectra of Rare Gas-Nitric Oxide van der Waals Molecules. Part 1. Theory of the Rotational Energy Levels. *J. Chem. Phys.* **1986**, *90*, 3331–3338.
- (13) Chhantyal-Pun, R.; Roudjane, M.; Melnik, D. G.; Miller, T. A.; Liu, J. Jet-Cooled Laser-Induced Fluorescence Spectroscopy of Isopropoxy Radical: Vibronic Analysis of B-X and B-A Band Systems. J. Phys. Chem. A 2014, 118, 11852.
- (14) Zu, L.; Liu, J.; Tarczay, G.; Dupré, P.; Miller, T. A. Jet-Cooled Laser Spectroscopy of the Cyclohexoxy Radical. *J. Chem. Phys.* **2004**, 120, 10579.
- (15) Liu, J.; Miller, T. A. Jet-Cooled Laser-Induced Fluorescence Spectroscopy of Cyclohexoxy: Rotational and Fine Structure of Molecules in Nearly Degenerate Electronic States. *J. Phys. Chem. A* **2014**, *118*, 11871.
- (16) Liu, J. Rotational and Fine Structure of Open-Shell Molecules in Nearly Degenerate Electronic States. *J. Chem. Phys.* **2018**, *148*, 124112.
- (17) Melnik, D.; Liu, J.; Curl, R. F.; Miller, T. A. Development of the Hamiltonian and Matrix Elements for Partially Deuterated Methoxy Radical. *Mol. Phys.* **2007**, *105*, 529.
- (18) Yan, Y.; Sharma, K.; Miller, T. A.; Liu, J. Rotational and Fine Structure of Open-Shell Molecules in Nearly Degenerate Electronic States. II. Interpretation of Experimentally Determined Interstate Coupling Parameters of Alkoxy Radicals. *J. Chem. Phys.* **2020**, *153*, 174306.
- (19) Gopalakrishnan, S.; Carter, C. C.; Zu, L.; Stakhursky, V.; Tarczay, G.; Miller, T. A. Rotationally resolved B-X electronic spectra

- of both conformers of the 1-propoxy radical. J. Chem. Phys. 2003, 118, 4954.
- (20) Gopalakrishnan, S.; Zu, L.; Miller, T. A. Rotationally Resolved Electronic Spectra of the $\tilde{B}-\tilde{X}$ Transition in Multiple Conformers of 1-Butoxy and 1-Pentoxy Radicals $\tilde{B}\tilde{X}$. J. Phys. Chem. A **2003**, 107, 5189
- (21) Brown, J. M.; Sears, T. J.; Watson, J. K. G. The Isotopic Dependence of the Spin-Rotation Interaction for an Asymmetric Top Molecule. *Mol. Phys.* **1980**, *41*, 173.
- (22) Brown, J. M.; Sears, T. J. A Reduced Form of the Spin-Rotation Hamiltonian for Asymmetric-Top Molecules, with Applications to HO₂ and NH₂. *J. Mol. Spectrosc.* **1979**, *75*, 111.
- (23) Liu, J.; Chen, M.-W.; Melnik, D.; Yi, J. T.; Miller, T. A. The spectroscopic characterization of the methoxy radical. I. Rotationally resolved Ã2A1–Ã2E electronic spectra of ÃX CH₃O. *J. Chem. Phys.* **2009**, 130, 074302.
- (24) Liu, J.; Chen, M.-W.; Melnik, D.; Miller, T. A.; Endo, Y.; Hirota, E. The Spectroscopic Characterization of the Methoxy Radical (Part II): Rotationally Resolved Ã2A1–Ã2E Electronic and Ã2E Microwave Spectra of the Perdeuteromethoxy Radical CD₃O. *J. Chem. Phys.* **2009**, *130*, 074303.
- (25) Liu, J.; Reilly, N. J.; Mason, A.; Miller, T. A. Laser-Induced Fluorescence Spectroscopy of Jet-Cooledt-Butoxy. *J. Phys. Chem. A* **2015**, *119*, 11804.
- (26) Mulliken, R. S.; Christy, A. Λ-Type Doubling and Electron Configurations in Diatomic Molecules. *Phys. Rev.* **1931**, 38, 87.
- (27) Curl, R. F. Microwave Spectrum of Chlorine Dioxide. III. Interpretation of the Hyperfine Coupling Constants Obtained in Terms of the Electronic Structure. *J. Chem. Phys.* **1962**, *37*, 779.
- (28) Hougen, J. T. Double Group Considerations, Jahn-Teller Induced Rovibronic Effects, and the Nuclear Spin-Electron Spin Hyperine Hamiltonian for a Molecule of Symmetry C_{3v} in an Electronic 2E State. *J. Mol. Spectrosc.* **1980**, *81*, 73.
- (29) Barckholtz, T. A.; Miller, T. A. Quantitative Insights About Molecules Exhibiting Jahn-Teller and Related Effects. *Int. Rev. Phys. Chem.* 1998, 17, 435.
- (30) Grütter, M.; Qian, X.; Merkt, F. Photoelectron spectroscopic study of the $E \otimes e$ Jahn-Teller effect in the presence of a tunable spin-orbit interaction. III. Two-state excitonic model accounting for observed trends in the \tilde{X}^2E ground state of CH 3X+(X=F, Cl, Br,I) and CH 3Y(Y=O,S). *J. Chem. Phys.* **2012**, *137*, 084313.
- (31) Maillard, J. P.; Chauville, J.; Mantz, A. W. High-resolution emission spectrum of OH in an oxyacetylene flame from 3.7 to 0.9 μ m. J. Mol. Spectrosc. **1976**, 63, 120–141.
- (32) Brooke, J. S. A.; Bernath, P. F.; Western, C. M.; Sneden, C.; Afşar, M.; Li, G.; Gordon, I. E. Line strengths of rovibrational and rotational transitions in the X²Π ground state of OH. *J. Quant. Spectrosc. Radiat. Transfer* **2016**, *168*, 142–157.
- (33) Holland, J. H. The Adaption in Natural and Artificial Systems; The University of Michigan Press: Ann Arbor, MI, 1975.
- (34) Goldberg, D. E. Genetic Algorithms in Search, Optimisation and Machine Learning; Addison-Wesley: Reading, MI, 1989.
- (35) Rechenberg, I. The Evolutionsstrategie: Optimierung technischer Systeme nach Prinzipien der biologischen Evolution; Frommann-Holzboog: Stuttgart, 1973.
- (36) Leo Meerts, W. L.; Schmitt, M. Application of Genetic Algorithms in Automated Assignments of High-Resolution Spectra. *Int. Rev. Phys. Chem.* **2006**, 25, 353.
- (37) Hageman, J. A.; Wehrens, R.; de Gelder, R.; Leo Meerts, W.; Buydens, L. M. C. Direct Determination of Molecular Constants from Rovibronic Spectra with Genetic Algorithms. *J. Chem. Phys.* **2000**, *113*, 7955.
- (38) Meerts, W. L.; Schmitt, M.; Groenenboom, G. C. New applications of the genetic algorithm for the interpretation of high-resolution spectra. *Can. J. Chem.* **2004**, 82, 804–819.
- (39) Stakhursky, V. L.; Miller, T. A. SpecView: Simulation and Fitting of Rotational Structure of Electronic and Vibronic Bands. *56th International Symposium on Molecular Spectroscopy*; The Ohio State

- University: Columbus, Ohio, 2001, TC06. https://louisville.edu/faculty/j0liu028/software/specview.
- (40) Zu, L.; Liu, J.; Gopalakrishnan, S.; Miller, T. A. The Rotationally Resolved Electronic Spectra of Several Conformers of 1-Hexoxy and 1-Heptoxy. *Can. J. Chem.* **2004**, 82, 854.
- (41) Just, G. M. P.; Rupper, P.; Miller, T. A.; Meerts, W. L. High-Resolution Cavity Ringdown Spectroscopy of the Jet-Cooled Ethyl Peroxy Radical C₂H₅O₂. *J. Chem. Phys.* **2009**, *131*, 184303.
- (42) Just, G. M. P.; Rupper, P.; Miller, T. A.; Meerts, W. L. High-Resolution Cavity Ringdown Spectroscopy of the Jet-Cooled Propyl Peroxy Radical C₃H₂O₂. *Phys. Chem. Chem. Phys.* **2010**, *12*, 4773.
- (43) Watson, J. K. G. Jahn-Teller and L-Uncoupling Effects on Rotational Energy Levels of Symmetric and Spherical Top Molecules. *J. Mol. Spectrosc.* **1984**, *103*, 125.
- (44) Liu, X.; Yu, L.; Miller, T. A. Jahn-Teller Induced Corrections to Rotational and Fine-Structure Parameters in Doubly Degenerate Electronic States. *J. Mol. Spectrosc.* **1990**, *140*, 112.
- (45) Jin, J.; Sioutis, I.; Tarczay, G.; Gopalakrishnan, S.; Bezant, A.; Miller, T. A. Dispersed Fluorescence Spectroscopy of Primary and Secondary Alkoxy Radicals. *J. Chem. Phys.* **2004**, *121*, 11780.